Electronic Supplementary Material (ESI) for Organic Chemistry Frontiers.

Barium cation-responsive supra-amphiphile constructed by new twisted cucurbit[15]uril/paraquat recognition in water

Qing Li, Jifu Sun, Jiong Zhou, Bin Hua, Li Shao, and Feihe Huang*

State Key Laboratory of Chemical Engineering, Center for Chemistry of High-Performance & Novel Materials,
Department of Chemistry, Zhejiang University, Hangzhou 310027, P. R. China; Fax and Tel: +86-571-8795-3189;
Email address: fhuang@zju.edu.cn.

Electronic Supplementary Information (8 pages)

1. Materials and methods

All reagents were commercially available and used as supplied without further purification. Solvents were either employed as purchased or dried according to procedures described in the literature. *t*Q[15] was prepared and purified according to a previously published method.[S1] NMR spectra were recorded with a Bruker Advance DMX 400 spectrophotometer or a Bruker Advance DMX 500 spectrophotometer with the deuterated solvent as the lock and the residual solvent or TMS as the internal reference. UV-vis spectroscopy was performed on a Shimadzu UV-2550 instrument at room temperature by using 1 cm quartz cells. The thermodynamic parameters and binding constant (K_a) for the inclusion complex of guest **G1** with *t*Q[15] were determined by titration calorimetry using a VP-ITC micro-calorimeter (Microcal, USA). The critical aggregation concentration (CAC) values of **G2** and *t*Q[15]⊃**G2** were determined on a DDS-307 instrument. Transmission electron microscopy (TEM) investigations were carried out on a JEM-1200EX instrument. Dynamic light scattering measurements were performed on a goniometer ALV/CGS-3 using a UNIPHASE He-Ne laser operating at 632.8 nm.

2. ^{1}H NMR spectrum of tQ[15]

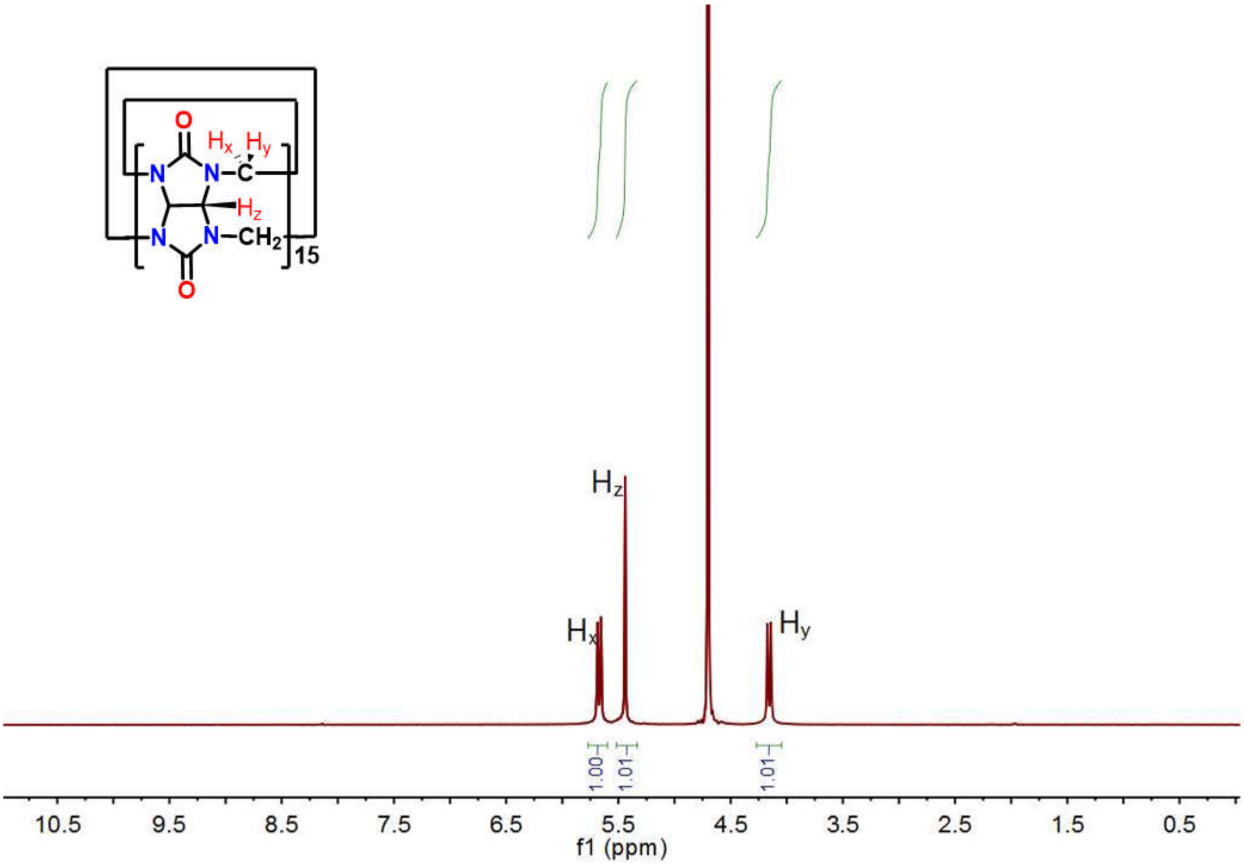

Figure S1. ^{1}H NMR spectrum (500 MHz, D_2O, 298 K) of *t*Q[15]

3. *Investigation of the interactions between **G1** and tQ[15]*

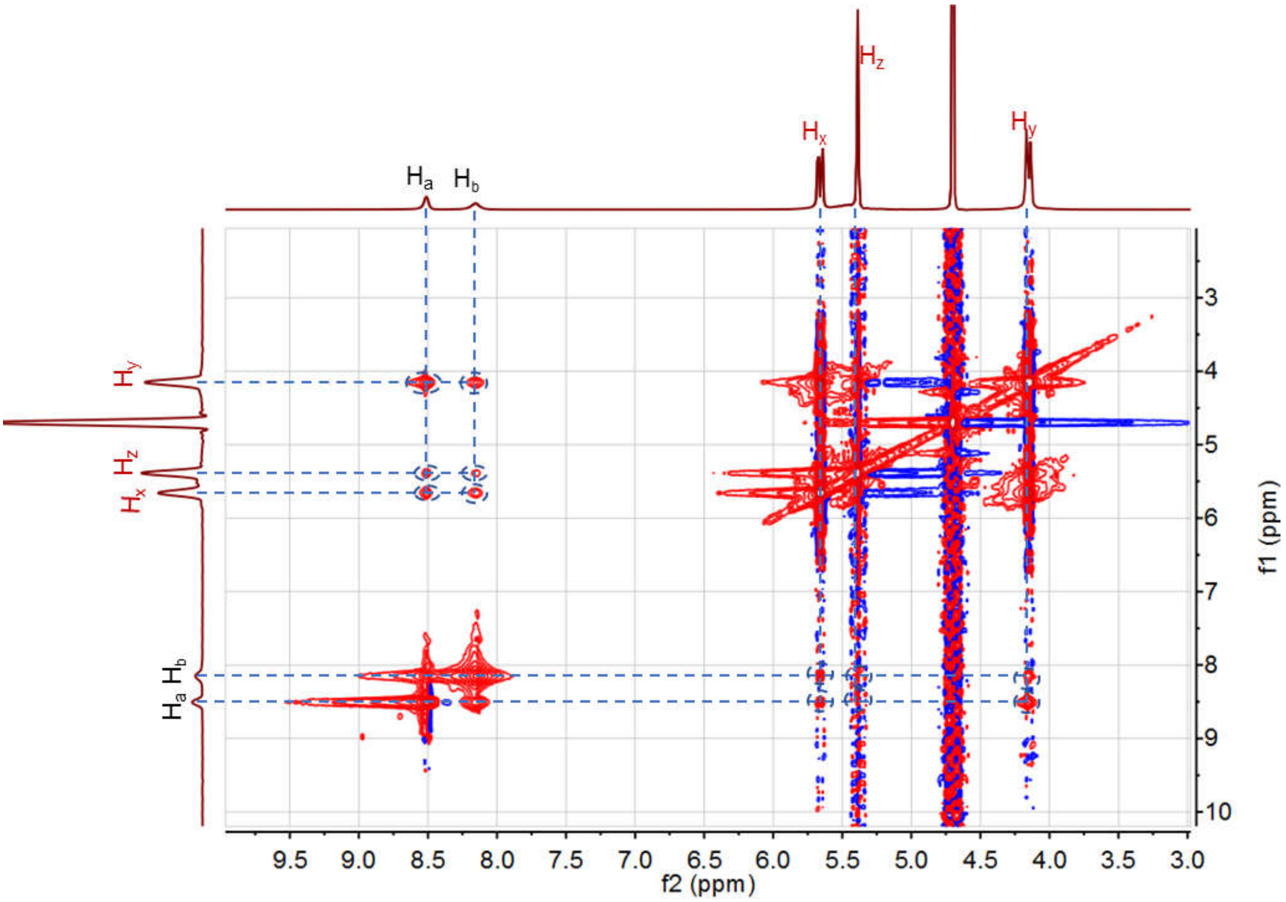

Figure S2. Partial 2D NOESY NMR spectrum (500 MHz, D_2O, 298 K) of *t*Q[15] (5.00 mM) and **G1** (25.0 mM).

*4. Isothermal titration calorimetry (ITC) experiments of tQ[15] with **G1** or Ba^{2+}*

The thermodynamic parameters and binding constant (K_a) for the inclusion complex of guest **G1** with *t*Q[15] or Ba^{2+} with *t*Q[15] were determined by titration calorimetry by using a VP-ITC micro-calorimeter (Microcal, USA). All solutions were prepared by using purified water and degassed prior to titration experiments. The heat evolved was recorded at T = 298 K. Computer simulations (curve fitting) were performed by using VP-ITC analytical software. The first data point was always removed from the data set prior to curve fitting. The data were analyzed with ORIGIN 8.0 software using the independent model.

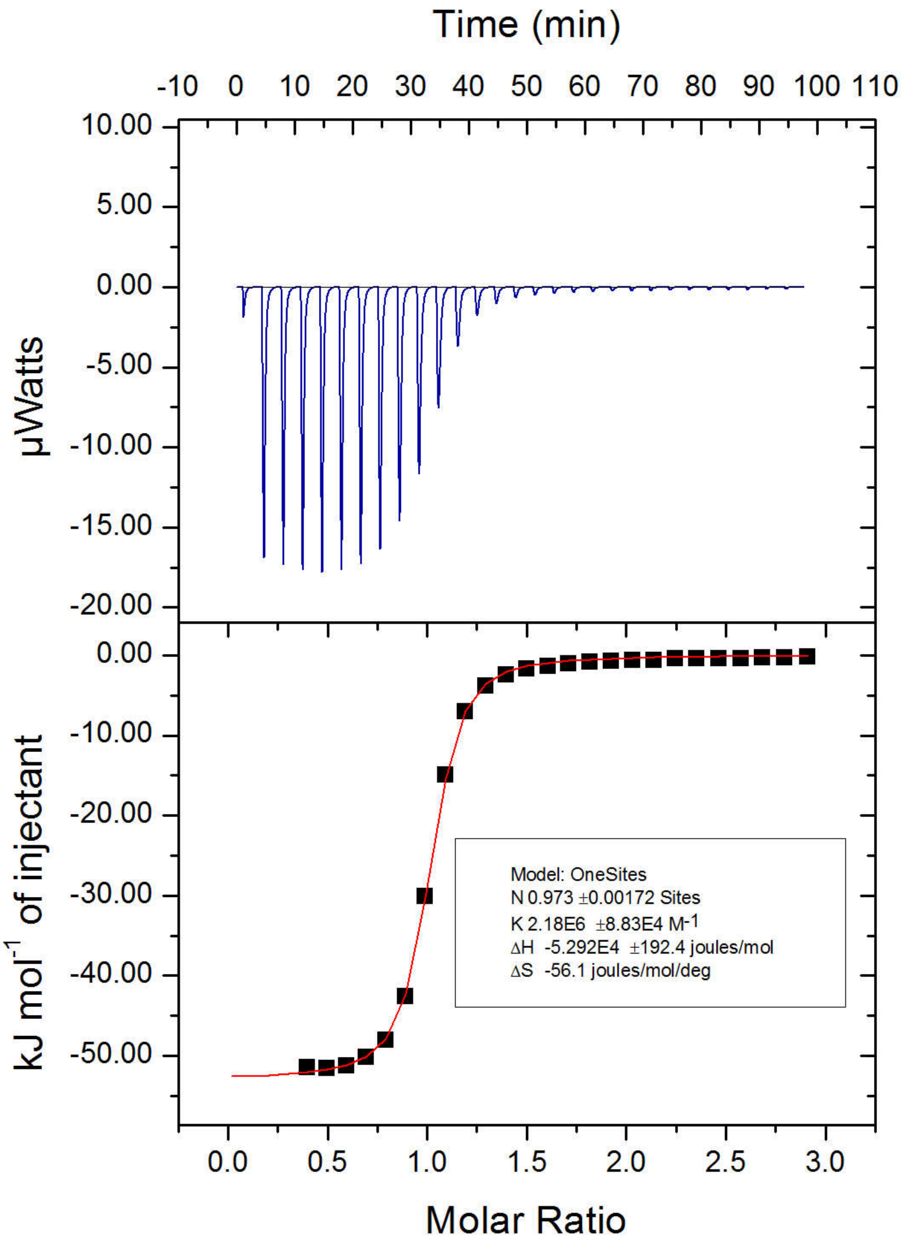

Figure S3. Microcalorimetric titration of *t*Q[15] with **G1** in water at 298 K. (Top) Raw ITC data for 29 sequential injections (10 μL per injection) of a **G1** solution (1.00 mM) into a *t*Q[15] solution (0.100 mM). (Bottom) Net reaction heat obtained from the integration of the calorimetric traces.

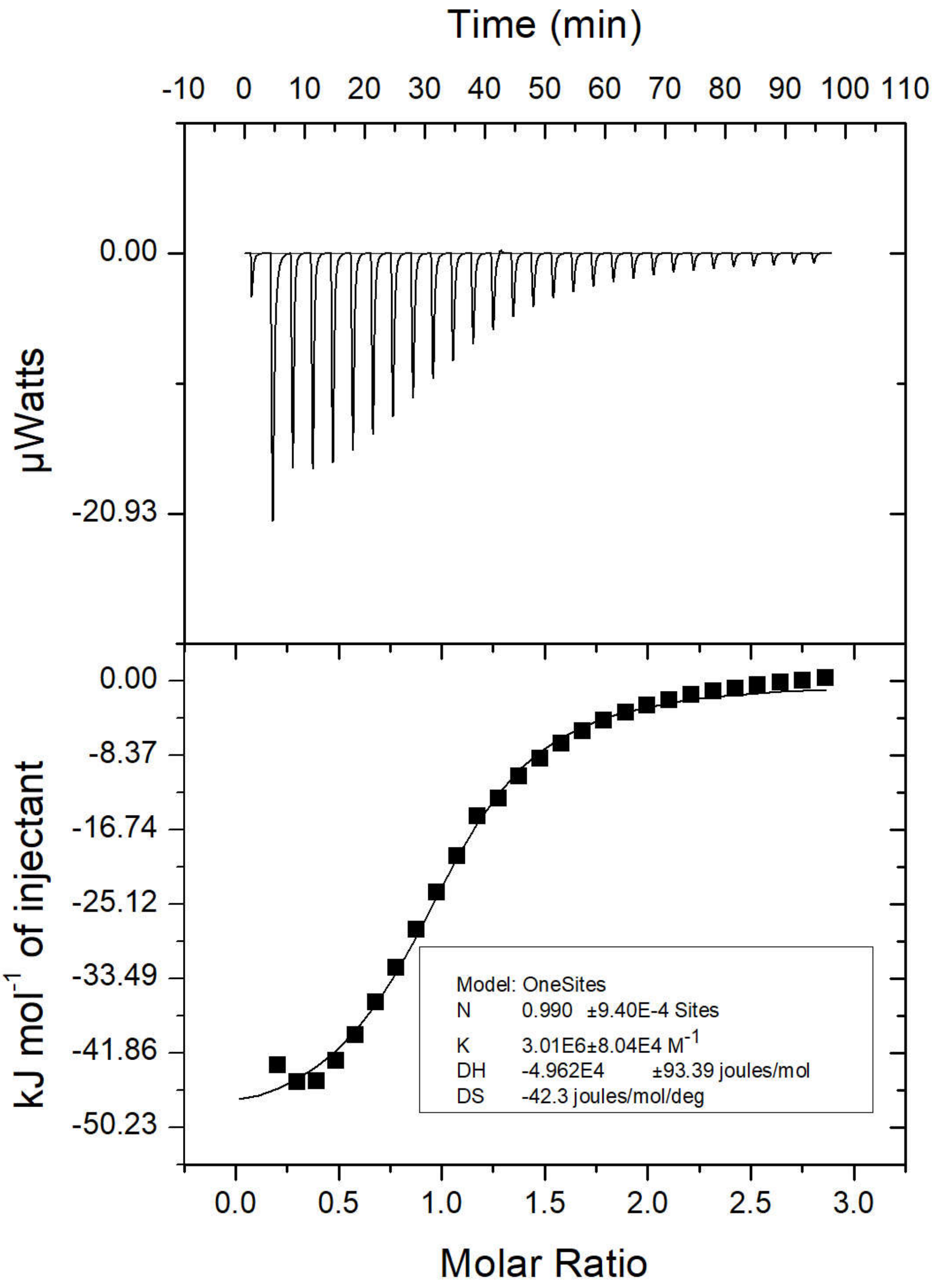

Figure S4. Microcalorimetric titration of *t*Q[15] with Ba^{2+} in water at 298 K. (Top) Raw ITC data for 29 sequential injections (10 μL per injection) of a Ba^{2+} solution (1.00 mM) into a *t*Q[15] solution (0.100 mM). (Bottom) Net reaction heat obtained from the integration of the calorimetric traces.

5. ^{1}H NMR spectra of barium cation-controlled complexation between tQ[15] and **G1**

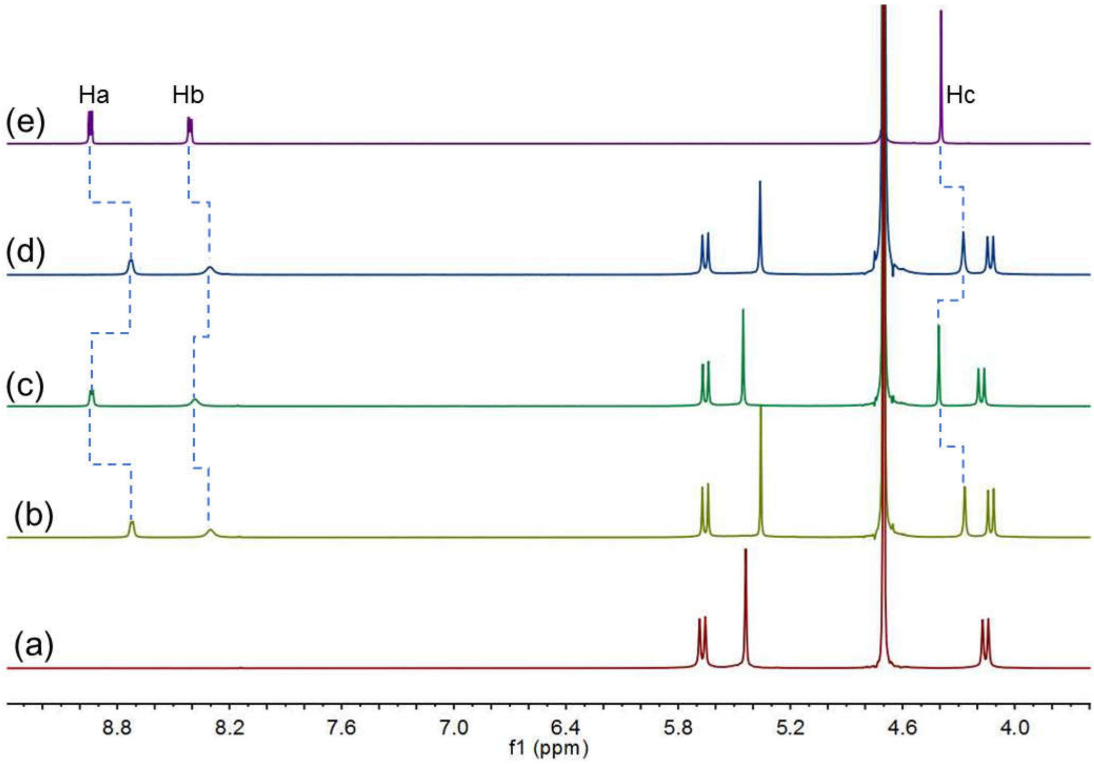

Figure S4. Partial ^{1}H NMR spectra (500 MHz, D_2O, 298 K): (a) 2.00 mM *t*Q[15]; (b) 2.00 mM *t*Q[15] and 10.0 mM $\mathbf{G_1}$; (c) after addition of 10 equiv of $BaCl_2$ to (b); (d) after addition of 10 equiv of Li_2SO_4 to (c); (e) 2.00 mM $\mathbf{G_1}$.

6. *Critical aggregation concentration (CAC) determination of **G2** and tQ[15]⊃**G2***

Some parameters such as the conductivity, fluorescence intensity, osmotic pressure and surface tension of the solution change sharply around the critical aggregation concentration. The dependence of the solution conductivity on the solution concentration is used to determine the critical aggregation concentration. Typically, the slope of conductivity versus the concentration below CAC is steeper than the slope above the CAC. Therefore, the junction of the conductivity-concentration plot represents the CAC value. To measure the CAC values of **G2** and *t*Q[15]⊃**G2** , the conductivities of the solutions at different concentrations were determined. By plotting the conductivity versus the concentration, we estimated the CAC values of **G2** and *t*Q[15]⊃**G2**.

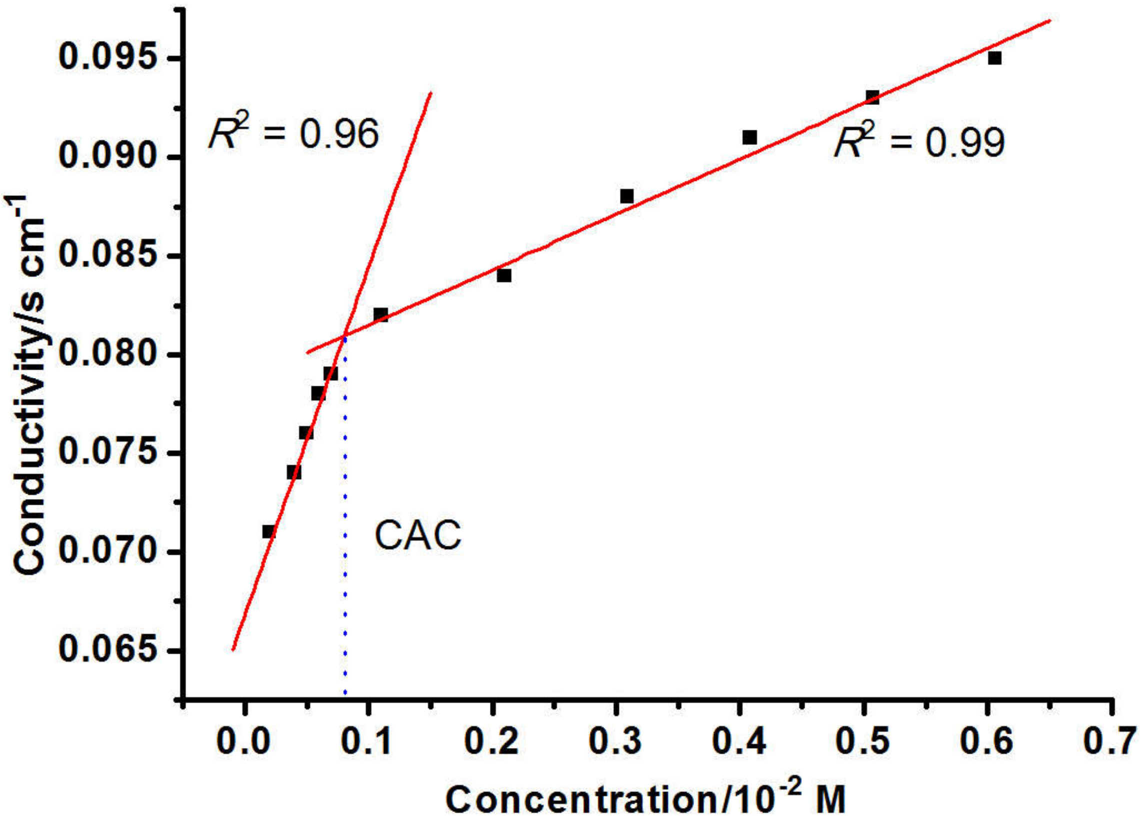

Figure S6. The concentration-dependent conductivity of **G2**. The critical aggregation concentration was determined to be (8.07 ± 0.21) × 10^{-4} M.

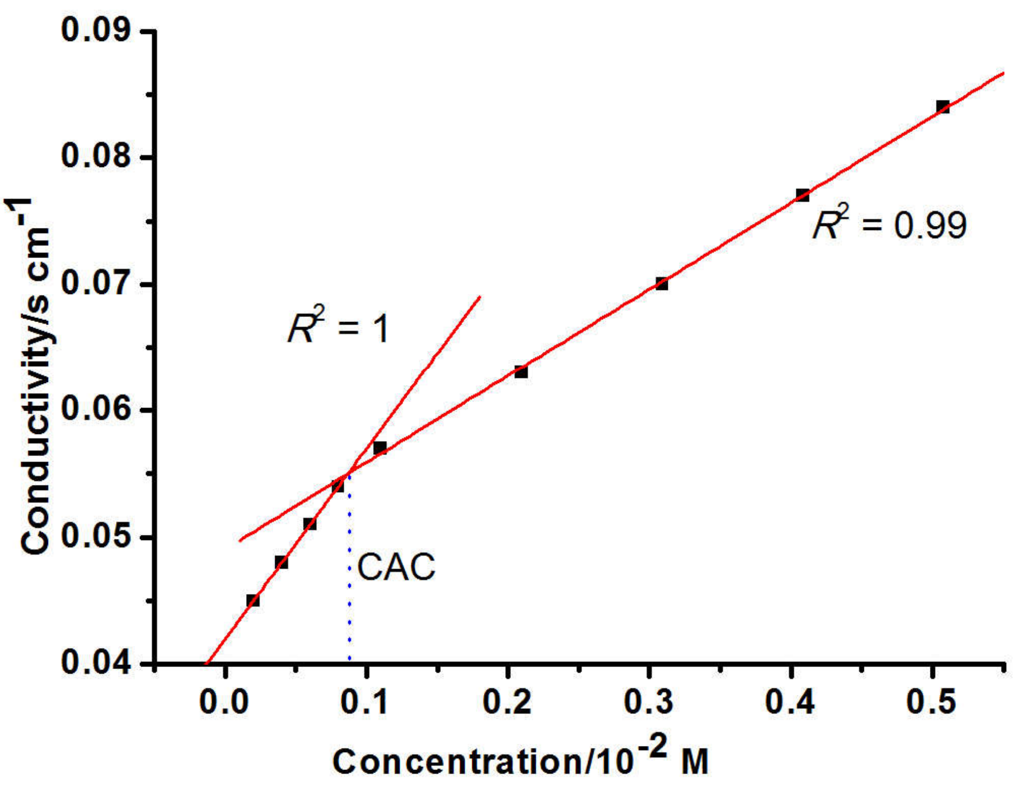

Figure S7. The concentration-dependent conductivity of *t*Q[15]$\supset$**G2**. The critical aggregation concentration (CAC) was determined to be (8.70 ± 0.14) × 10^{-4} M.

7. Size information of the molecular model of ***G2***

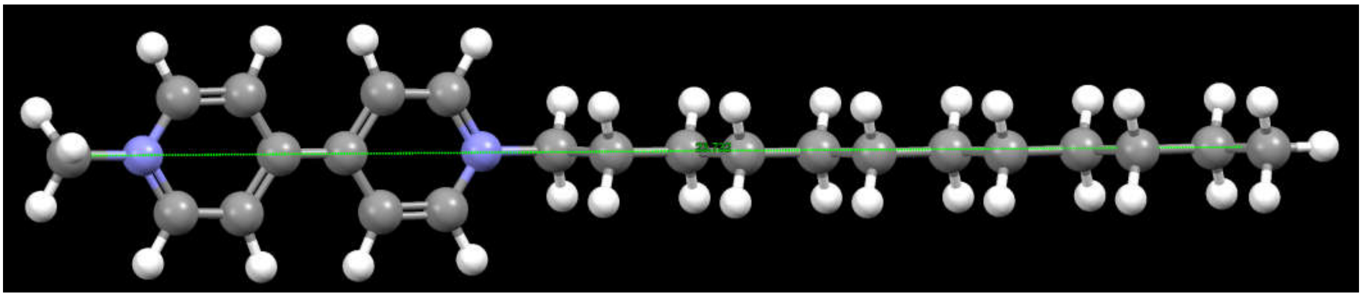

Figure S8. The energy-minimized structure of **G2** obtained from ChemBio 3D Ultra 14.0 and Mercury 1.4.1. Iodide anion and bromide anion were omitted for clarity. The length of **G2** molecule was calculated to be about 2.4 nm.

8. *UV-vis spectroscopy investigation of tQ[15]/**G1** with Ba^{2+}, Mg^{2+}, Ca^{2+} and Sr^{2+}.*

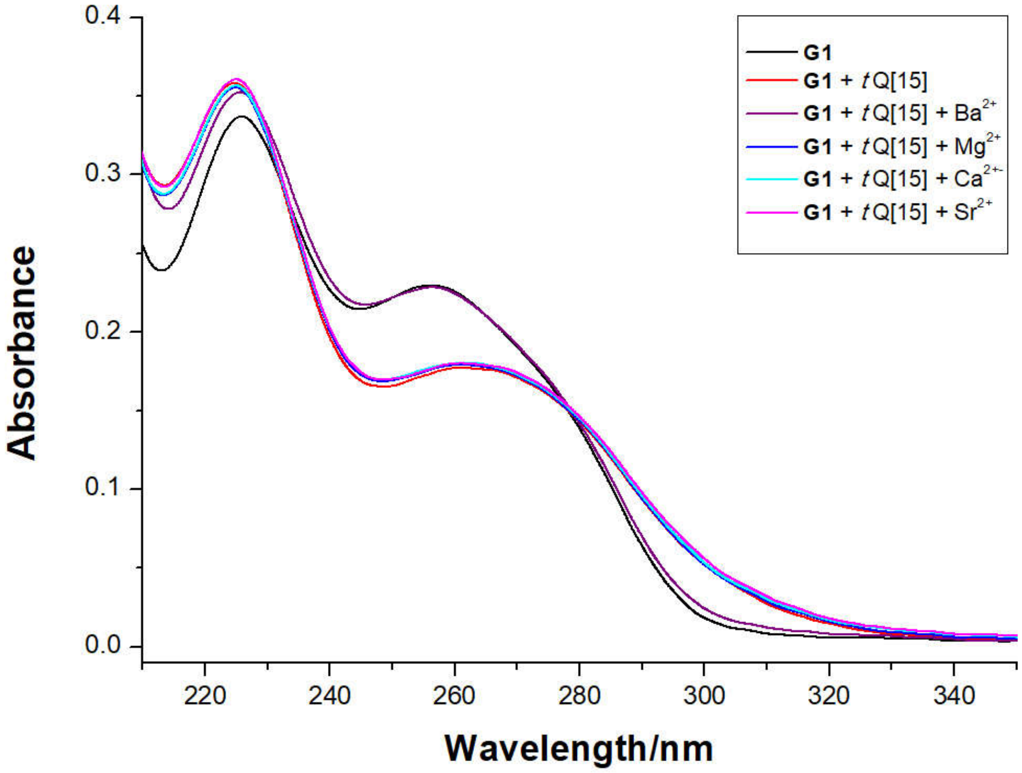

Figure S9. Absorption spectra of 10.0 mM **G1**, 10.0 mM *t*Q[15] + 10.0 mM **G1**, 10.0 mM *t*Q[15] + 10.0 mM **G1** + 100 mM Ba^{2+}, 10.0 mM *t*Q[15] + 10.0 mM **G1** + 100 mM Mg^{2+}, 10.0 mM *t*Q[15] + 10.0 mM **G1** + 100 mM Ca^{2+} and 10.0 mM *t*Q[15] + 10.0 mM **G1** + 100 mM Sr^{2+} in water.

References:

S1. Q. Li, S. Qiu, J. Zhang, K. Chen, Y. Huang, X. Xiao, Y. Zhang, F. Li, Y. Zhang, S. Xue, Q. Zhu, Z. Tao, L. F. Lindoy and G. Wei, *Org. Lett.*, 2016, **18**, 4020.